MAiNTENANCE
The University of Manchester

Proceedings of 1st International Conference on Maintenance Engineering, IncoME-I 2016
The University of Manchester, UK

Paper No ME2016_xxxx

Frictional Effects on the Diagnostics of Helical Gear Tooth Defects

Khaldoon F. Brethee[1], Xiaojun Zhou[2], Fengshou Gu[1], Andrew D. Ball[1]

[1]Centre for Efficiency and Performance Engineering, University of Huddersfield, Huddersfield, HD1 3DH.

[2]China Ship Research and Development Academy, Beijing PR China 100192

Email: khaldoon.brethee@hud.ac.uk; xiaojun.zhou.cqu@gmail.com; F.Gu@hud.ac.uk; A.Ball@hud.ac.uk

Abstract Tooth Defect is a common failure mode that frequently occurs in gears. To develop successful diagnostic techniques, this study examines the capability of helical gear dynamic responses with the inclusion of different time-varying friction models, i.e. friction-free, Coulomb and elasto-hydrodynamic lubrication (EHL) models. The gear system is a 10-DOF (degree-of-freedom) vibration system, which incorporates the effects of gear pair, supporting bearings, driving motor and loading system. Moreover, it couples the transverse and torsional motions resulting from time-varying friction forces, time varying mesh stiffness excitations and different tooth breakage severities. To explore the vibration response, spectral peaks at characteristic mesh frequency and its harmonics along with their sidebands are considered in the light of the impulsive sources from tooth damages and different frictional excitation models. It has found that the sidebands exhibit significant difference between different friction models and mesh components for tooth defects. It is concluded that the frictional effect should be taken into account if it is to be an accurate method for the detection and diagnostic different tooth surface defects.

Key words Diagnostics, Frictional effect, Helical gear system, Tooth breakage.

1.0 Introduction

Gears are very important element in a variety of industrial applications such as helicopters, marine power trains, wind turbine, cranes etc. However, the investable friction between contact tooth surfaces may be the root that leads to various unexpected failures such as wear, scuffing, pitting and even tooth breakage. In the meantime, this frictional effect and change may cause different gear vibration characteristics. Therefore, in-depth understandings of gear vibrations accounting frictional effects need to be gained in order to find early signs of friction induced incipient fault and take correct maintenance produced to prevent serious failure consequences.

A comprehensive literature review shows that modelling gear dynamics is a main stream approaches in understanding gear vibrations. Different dynamic models for various gearbox systems were presented in [1-4], in which both torsional and translational vibration responses of gears were studied as a tool for aiding gearbox diagnostic inferences such as gear spalling or tooth breakage [5, 6], tooth crack [7-9], tooth surface pitting and wear [10, 11]. In addition, tooth friction was demonstrated as a non-negligible excitation source in gear vibration and noise [12-15]. However, most of the presented models ignored the friction effect or did not consider the friction between gear tooth contacts effectively in studying the diagnostic features, which may give less concentration of diagnostic results. Moreover, most of the earlier researches focused on spur gears than the helical gears due to the existence of helix angle that increases number and length of time-varying contact lines.Recently, several studies have been carried to develop analytical methods for investigating helical gear stiffness model. Kar and Mohanty [16, 17] suggested an algorithm for determination of time-varying stiffness and time varying frictional force and torque at meshing teeth and the bearings in a helical gear system. This algorithm was revised and refined by Jiang et al. [12, 18] to develop more accurate representations of stiffness variations of helical gears during the mesh process. However, these models were presented by assuming constant friction coefficient, which may different from the real applications in that the load and hence the frictional forces vary during the meshing process.

The main objective of this study is to increase the capability of conventional modelling of helical gear systems for providing accurate diagnostic determinations. The model is developed with the inclusion of different time varying frictional models such as friction-free, Coulomb friction and EHL models. The gear vibration signatures due to different tooth breakage severities are obtained to evaluate the effect of different frictional excitations and improve diagnostic performance for different tooth surface defects.

2.0 Helical Gear Mesh Stiffness

Since, time-varying stiffness is the main source of gear vibration, whereas dynamic measurements have been verified that the mesh stiffness of a helical gear is roughly proportional to the sum of the lengths of the contact lines of all the tooth pairs in contact [19]. The contact line for a helical gear pair can be determined from the kinematic compatibility between the numerically generated surfaces of the teeth in contact as expressed by Kar and Mohanty [16, 17] and subsequently modified by Jiang [12]. Based on these researches, the overall stiffness function is defined as a combination of all meshing tooth pairs,

$$K_{mi}(t) = k_0 \; L_i(t) \tag{1}$$

where $L_i(t)$ is the total length of contact lines during the gear mesh process and k_0 is a mesh stiffness density per unit length. However, loss on tooth is reflected mainly in lack of tooth's stiffness relating to its damage severity [5, 6]. Tooth damage is represented by taking into account the geometric changes due to the tooth breakage. Figure 1 shows the time varying of meshing stiffness with different tooth breakage severities (50%, and 100% tooth breakage (TB)). The gear meshing process is interrupted by the faulty tooth through local stiffness drops which leads to additional impacts between the driven and driving gears.

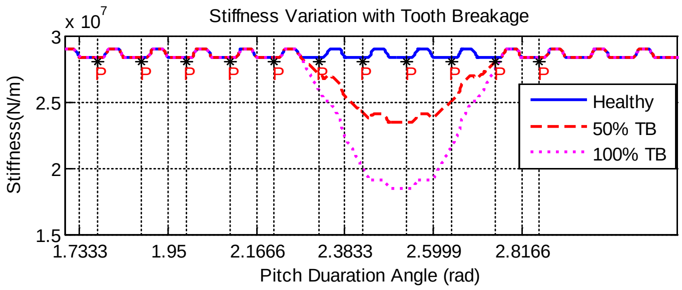

Figure 1 Time-varying mesh stiffness variations with different tooth breakages

3.0 Friction Coefficient Models

Many parameters affect friction coefficient μ between gear meshing surfaces due to the complex gear lubricating mechanisms. Therefore, researchers have proposed different empirical formulae to estimate the friction coefficient [20]. Consequently, the assumption of constant normal force and constant friction coefficient may not lead to a realistic result [12]. For the purpose of explanation, the coefficient of friction is represented as an idealized mathematical entity. Different friction coefficient model are used in this study, free-friction, constant friction coefficient and EHL models as shown in Figure 2. The constant friction coefficient is defined as the mean value of EHL. In general, the theoretical friction coefficient is derived from EHL and tribology theory, which was considered as the dominant mode of lubrication accumulated with the gears meshing surfaces [21], which was proposed by Xu et al. [20], i.e.

$$\mu = f\left(v_k, v_o, V_s, V_r, R, W, P_{\max}, S, \ldots\right) \tag{2}$$

where v_k and v_o are the kinematic and dynamic viscosities of lubricant, V_s is the relative sliding velocity, V_r is the sum of the rolling velocities, R is the combined radius of curvature, W is the unit normal load, P_{max} is the maximum contact pressure and S is the surface roughness parameter.

$$\mu = e^{f(SR, P_h, \upsilon_o, S)} P_h^{b2} \left|SR\right|^{b3} V_e^{b6} v_0^{b7} R^{b8} \tag{3}$$

$$f(SR, P_h, \upsilon_o, S) = b1 + b4\left|SR\right| P_h \log_{10}(\upsilon_o) + b5e^{-\left|SR\right| P_h \log_{10}(\upsilon_o)} + b9e^{S} \tag{4}$$

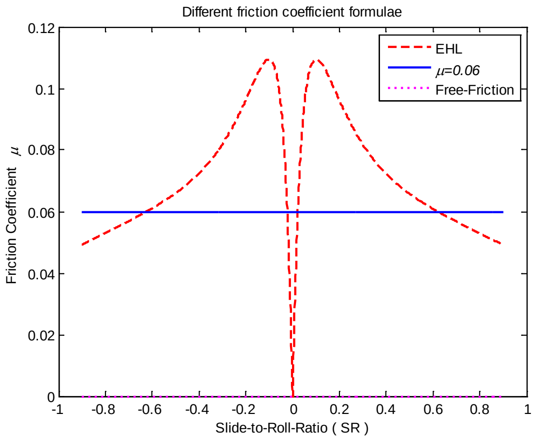

Figure 2 Different model of friction coefficient.

4.0 Modelling of a Helical Gear Transmission System

Numerical model is an effective method that is widely used to simulate gear vibrations under different operating conditions. It can simplify the development of diagnostic and prognostic techniques in real systems, whereas high reliability for early detection of incipient gear failure can be achieved. In terms of the prediction of interfacial friction forces in helical gear dynamic models, a 10-DOF nonlinear model is proposed based on Refs. [12, 16, 18] to model gear pair in mesh connected to load (T_L) and motor (M_m) by two shafts, which are simulated by torsional stiffness and torsional damping components (k_1, k_2, c_1 and c_2), as shown in Figure 3. The gears (p represents pinion and g represents gear) have geometric properties illustrated in Table 1. They coupled by a non-linear spring having time varying mesh stiffness K_m *(t)* and a varying mesh damping C_m *(t)*. The model includes four inertias, namely load, motor, pinion and gear. The torsional compliances of shafts and the transverse compliances of bearings combined with those of shafts are included in the model. The resilient elements of supports are described by stiffness and damping coefficients K_{x1}, K_{x2}, C_{x1} and C_{x2} for the pinion and gear respectively in the OLOA direction, besides K_{y1}, K_{y2}, C_{y1} and C_{y2} in the LOA direction, similarly K_{z1}, K_{z2}, C_{z1} and C_{z2} in the axial direction. Each gear was represented by rigid blocks with four degree of freedom (three translations and one rotation). The governing equations of motion for the model depicted in Figure 3 was written depend on the following key assumptions:

- Pinion and gear are modelled as rigid disks;
- Shaft mass and inertia are lumped at the gears;
- Helical gear teeth are assumed to be perfectly involute and the manufacturing and assembly errors are ignored;
- Backlash is not considered in this model, thus there is no tooth separation.

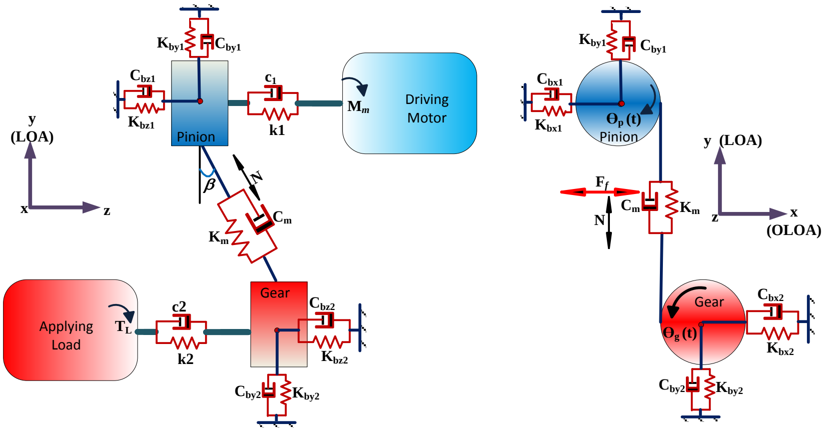

Figure 3 Schematic diagram of helical gear system

According to the Newtonian law of motion the equations of the motion are:

$$I_m\ddot{\theta}_{in} + c_1\left(\dot{\theta}_{in} - \dot{\theta}_p\right) + k_1\left(\theta_{in} - \theta_p\right) = M_m \tag{5}$$

$$\begin{aligned} I_p\ddot{\theta}_p - c_1\left(\dot{\theta}_{in} - \dot{\theta}_p\right) - k_1\left(\theta_{in} - \theta_p\right) + r_{bp}C_m(t)\left(r_{bp}\dot{\theta}_p - r_{bg}\dot{\theta}_g + \dot{y}_p - \dot{y}_g\right) \\ + r_{bp}K_m\left(t\right)\left(r_{bp}\theta_p - r_{bg}\theta_g + y_p - y_g\right) + T_{fp} = 0 \end{aligned} \tag{6}$$

$$\begin{aligned} I_g\ddot{\theta}_g + c_2\left(\dot{\theta}_g - \dot{\theta}_{out}\right) + k_1\left(\theta_g - \theta_{out}\right) - r_{bg}C_m(t)\left(r_{bp}\dot{\theta}_p - r_{bg}\dot{\theta}_g + \dot{y}_p - \dot{y}_g\right) \\ - r_{bg}K_m\left(t\right)\left(r_{bp}\theta_p - r_{bg}\theta_g + y_p - y_g\right) - T_{fg}\left(t\right) = 0 \end{aligned} \tag{7}$$

$$I_L\ddot{\theta}_{out} - c_2\left(\dot{\theta}_g - \dot{\theta}_{out}\right) - k_1\left(\theta_g - \theta_{out}\right) = -T_L \tag{8}$$

$$\begin{aligned} m_p\ddot{y}_p + C_m(t)\cos\beta_b\left(r_{bp}\dot{\theta}_p - r_{bg}\dot{\theta}_g + \dot{y}_p - \dot{y}_g\right) + \\ K_m(t)\cos\beta_b\left(r_{bp}\theta_p - r_{bg}\theta_g + y_p - y_g\right) + C_{by1}\dot{y}_p + K_{by1}y_p = 0 \end{aligned} \tag{9}$$

$$\begin{aligned} m_g\ddot{y}_g - C_m(t)\cos\beta_b\left(r_{bp}\dot{\theta}_p - r_{bg}\dot{\theta}_g + \dot{y}_p - \dot{y}_g\right) - \\ K_m(t)\cos\beta_b\left(r_{bp}\theta_p - r_{bg}\theta_g + y_p - y_g\right) + C_{by2}\dot{y}_g + K_{by2}y_g = 0 \end{aligned} \tag{10}$$

$$m_p\ddot{z}_p + C_m(t)\sin\beta_b[\dot{z}_p - \dot{z}_p + \tan\beta_b(r_{bp}\dot{\theta}_p - r_{bg}\dot{\theta}_g + \dot{y}_p - \dot{y}_g)] + \\ K_m(t)\sin\beta_b[z_p - z_g + \tan\beta_b(r_{bp}\theta_p - r_{bg}\theta_g + y_p - y_g)] + C_{bz1}\dot{z}_p + K_{bz1}z_p = 0 \tag{11}$$

$$m_g\ddot{z}_g - C_m(t)\sin\beta_b[\dot{z}_p - \dot{z}_p + \tan\beta_b(r_{bp}\dot{\theta}_p - r_{bg}\dot{\theta}_g + \dot{y}_p - \dot{y}_g)] - \\ K_m(t)\sin\beta_b[z_p - z_g + \tan\beta_b(r_{bp}\theta_p - r_{bg}\theta_g + y_p - y_g)] + C_{bz2}\dot{z}_g + K_{bz2}z_g = 0 \tag{12}$$

$$m_p\ddot{x}_p + C_{bx1}\dot{x}_p + K_{bx1}x_p - F_f = 0 \tag{13}$$

$$m_g\ddot{x}_g + C_{bx2}\dot{x}_g + K_{bx2}x_g + F_f = 0 \tag{14}$$

Table 1 The main properties of helical gear system

Parameters	Pinion	Gear
Number of teeth	Z_1=58	Z_2=47
Base radii (mm)	r_{bp}=37.663	r_{bg}=30.52
Gear mass (kg)	m_p=0.9	m_g=0.58
Normal module (mm)	1.25	
Pressure angle α (°)	20	
Face width b (mm)	25	
Helix angle β_b (°)	27	
Contact ratio ε_a	1.652	
Overlap ratio ε_b	2.89	

5.0 Results and Discussions

5.1 Time and Frequency Domain Analyses

Time and frequency domain analyses are commonly used to highlight the impulsive vibration of tooth breakage [6]. Figure 4 shows the translational raw data and its spectra for healthy and 100% tooth breakage obtained under three model cases. It can be seen in Fig.4 (a) and (b) that amplitudes at corresponding mesh frequencies are higher for the cases where the friction are on effect. Moreover, for the tooth breakage, the signals have significant local pulses in the time domain in Fig. 4(c) and show richness of frequency components, of which many can be correlated with the mesh components in the form of sidebands even though there are several distinctive local spectral clusters due to system resonances, as shown in Fig. 4(d). In addition, the friction also makes the corresponding amplitude higher.

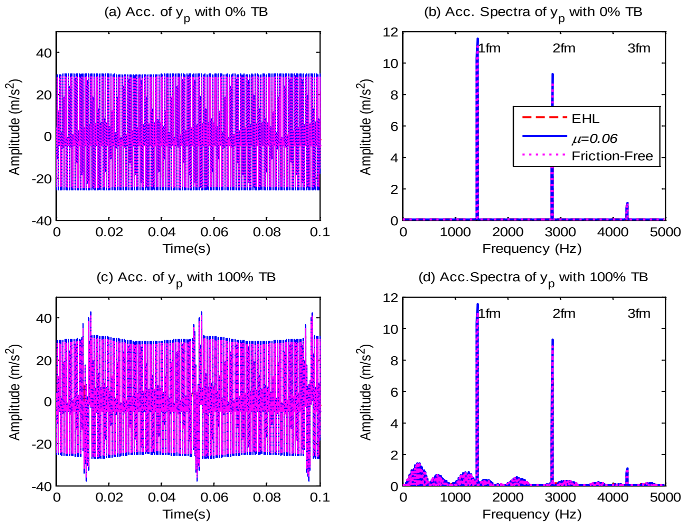

Figure 4 Raw data and spectral for healthy and 100% tooth breakage

5.2 Vibration Amplitude at Mesh Frequency Components

The amplitude of vibration signal at the mesh frequency and its harmonics are used to evaluate the effect of tooth breakage and friction on the gear transmission responses. The spectral peak values of the first three harmonics of the mesh frequency are represented in Figure 5. It can be seen that there is a clear difference in the influence for the first harmonic, in which the spectral peaks of EHL friction model shows an increase influences due to the impulsive duration of tooth breakages while the other models behave inconsistently. In addition, same trends can be found for all friction models at the second and third harmonics; however, the biggest influence can be demonstrated within the EHL model. Therefore, friction should be considered effectively in the dynamic model when the spectral at meshing components are used for detection and diagnostics gear surface faults.

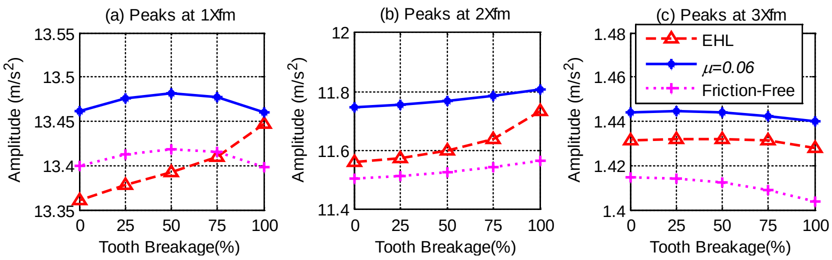

Figure 5 Spectral peaks at meshing components

5.3 Vibration Amplitude at Sideband Frequencies

While a local defect such as tooth breakage and cracks etc occurred, the gear vibration responses exhibit with additional impulsive components, which results in more amplitude and phase modulation to the gear meshing components. The dynamic response shows that the presence of sidebands around the gear mesh frequency and its harmonics are caused by a local stiffness decrease [5]. The spectral peaks of the lower and upper sideband frequencies ($f_{sb} = f_m \mp f_r$) of the meshing frequency components are shown in Figure 6.

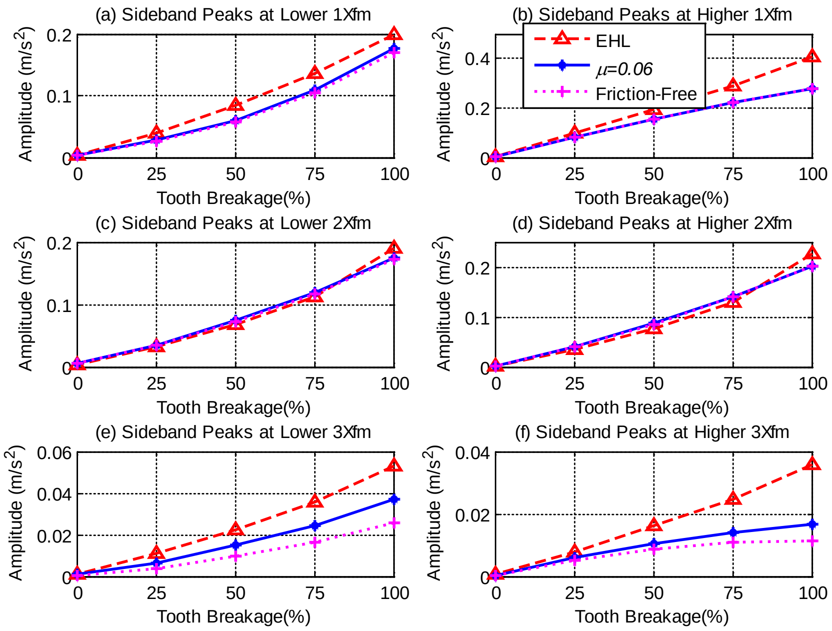

Figure 6 Spectral peaks of sidebands at the mesh frequency components

It can be seen that all sideband peaks are generally increased with the tooth breakage severity. However, the most influential increase can be identified with the EHL friction model, whereas the sidebands around the 3rd harmonic show a very clear difference. It could enhance by more than 50% as compared with the friction-free, which can show significant influences on the diagnostic features. In addition, the EHL friction model cause slight increase on the sidebands of the first meshing component and little change to that of the second mesh harmonic. Therefore, based on the sideband changes, the break tooth can be diagnosed and based on the difference of change rate, lubrication conditions could be evaluated.

6.0 Conclusion

This study investigates the frictional effects on helical gear dynamic response with the inclusion of different tooth breakage severities. To increase the capability of conventional models in developing accurate diagnostics features, frictional effects are accounted in conventional vibration models. In particular, vibration responses are investigated under friction-free, Coulomb and EHL friction models. Key diagnostic features such as spectral peaks at mesh frequency components and sidebands are compared and they show significant changes in the response patterns due to impulsive sources of tooth breakage and different frictional excitation models. The results show that spectral peaks are generally increased with doubled sideband amplitudes at the third mesh components and less changes appearing around the second mesh harmonic. However, the EHL model produces the most influence than the others upon these features. In the same time, the amplitudes at the mesh frequency components also show more consistent influence with the tooth breakages for the EHL model. In addition, the difference of sideband change rates among different mesh components can offer information about gear lubrication conditions. These findings have confirmed that friction contributions should be considered effectively in the gear dynamic model to obtain accurate diagnostic results for tooth surface defects.

Reference

[1] Begg, C.D., et al. *Dynamics modeling for mechanical fault diagnostics and prognostics*. in *Maintenance and Reliability Conf*. 1999.

[2] Bruns, C.J., *Dynamic gearbox simulation for fault diagnostics using a torque transducer*. 2011.

[3] Bartelmus, W., *Mathematical modelling and computer simulations as an aid to gearbox diagnostics.* Mechanical Systems and Signal Processing, 2001. **15**(5): p. 855-871.

[4] Van Khang, N., T.M. Cau, and N.P. Dien, *Modelling parametric vibration of gear-pair systems as a tool for aiding gear fault diagnosis.* technische mechanik, 2004. **24**: p. 3-4.

[5] Chaari, F., et al., *Effect of spalling or tooth breakage on gearmesh stiffness and dynamic response of a one-stage spur gear transmission.* European Journal of Mechanics-A/Solids, 2008. **27**(4): p. 691-705.

[6] Jia, S. and I. Howard, *Comparison of localised spalling and crack damage from dynamic modelling of spur gear vibrations.* Mechanical Systems and Signal Processing, 2006. **20**(2): p. 332-349.

[7] Tian, Z., M.J. Zuo, and S. Wu, *Crack propagation assessment for spur gears using model-based analysis and simulation.* Journal of Intelligent Manufacturing, 2012. **23**(2): p. 239-253.

[8] Wu, S., M.J. Zuo, and A. Parey, *Simulation of spur gear dynamics and estimation of fault growth.* Journal of Sound and Vibration, 2008. **317**(3): p. 608-624.

[9] Mohammed, O.D., et al., *Vibration signal analysis for gear fault diagnosis with various crack progression scenarios.* Mechanical systems and signal processing, 2013. **41**(1): p. 176-195.

[10] Ding, H., *Dynamic Wear Models for Gear Systems*. 2007, The Ohio State University.

[11] Flodin, A., *Wear of spur and helical gears.* Royal Institute of Technology, Stockholm, Doctoral Thesis, 2000.

[12] Jiang, H., *Analysis of time-varying friction excitations in helical gears with refined general formulation.* Proceedings of the Institution of Mechanical Engineers, Part C: Journal of Mechanical Engineering Science, 2015: p. 0954406215583886.

[13] Velex, P. and P. Sainsot, *An analytical study of tooth friction excitations in errorless spur and helical gears.* Mechanism and Machine Theory, 2002. **37**(7): p. 641-658.

[14] He, S., R. Gunda, and R. Singh, *Inclusion of sliding friction in contact dynamics model for helical gears.* Journal of mechanical design, 2007. **129**(1): p. 48-57.

[15] Brethee, K.F., et al. *Analysis of frictional effects on the dynamic response of gear systems and the implications for diagnostics*. in *Automation and Computing (ICAC), 2015 21st International Conference on*. 2015. IEEE.

[16] Kar, C. and A. Mohanty, *An algorithm for determination of time-varying frictional force and torque in a helical gear system.* Mechanism and machine theory, 2007. **42**(4): p. 482-496.

[17] Kar, C. and A. Mohanty, *Determination of time-varying contact length, friction force, torque and forces at the bearings in a helical gear system.* Journal of Sound and Vibration, 2008. **309**(1): p. 307-319.

[18] Jiang, H., Y. Shao, and C.K. Mechefske, *Dynamic characteristics of helical gears under sliding friction with spalling defect.* Engineering Failure Analysis, 2014. **39**: p. 92-107.

[19] Kang, J.S. and Y.-S. Choi, *Optimization of helix angle for helical gear system.* Journal of mechanical science and technology, 2008. **22**(12): p. 2393-2402.

[20] Xu, H., *Development of a generalized mechanical efficiency prediction methodology for gear pairs.* 2005, The Ohio State University.

[21] Hamel, M.A., *Condition monitoring of helical gears using acoustic emission (AE) technology.* 2013.

Authors’ Biography

	**Khaldoon F. Brethee** **Khaldoon F. Brethee** is currently a Ph.D. student at Centre for Efficiency and Performance Engineering (CEPE), University of Huddersfield, UK. He is a member staff at University of Al-Anbar, Iraq. His research interests include gear dynamic vibrations and fault diagnostics.
	**Xiaojun Zhou** **Dr Xiaojun Zhou** is a senior visiting scholar at CEPE, University of Huddesfield, UK. He is working on a project of vibration-based ship power train condition monitoring.
	**Fengshou Gu** **Dr Fengshou Gu** is a principle researcher fellow, Head of Measurement and Data Analysis Group. He experts in the fields of vibro-acoustics analysis and machinery diagnosis, He is the author of over 200 technical and professional publications in machine dynamics, signal processing, condition monitoring and related fields.
	**Andrew D. Ball** **Prof Andrew Ball** is the director of CEPE. He expertises in the detection and diagnosis of faults in mechanical, electrical and electro-hydraulic machines and published over 250 technical and professional publications.